Title

Complement factor H genotypes impact risk of age-related macular degeneration by interaction with oxidized phospholipids

Journal

Proceedings of the National Academy of Sciences of the United States of America, 109(34)

ISSN

0027-8424

Authors

Shaw, Peter X
Zhang, Li
Zhang, Ming
et al.

Publication Date

2012-08-21

DOI

10.1073/pnas.1121309109

Peer reviewed

Complement factor H genotypes impact risk of age-related macular degeneration by interaction with oxidized phospholipids

Peter X. Shaw[a,b,c], Li Zhang[b,c], Ming Zhang[a], Hongjun Du[a,b,c], Ling Zhao[a,b,c], Clara Lee[b,c], Seanna Grob[b,c], Siok Lam Lim[b,c], Guy Hughes[b,c], Janet Lee[b,c], Matthew Bedell[b,c], Mark H. Nelson[d], Fang Lu[a], Martin Krupa[b,c], Jing Luo[b,c], Hong Ouyang[b,c], Zhidan Tu[e], Zhiguang Su[a], Jin Zhu[a,b,c], Xinran Wei[a,b,c], Zishan Feng[f], Yaou Duan[a,b,c], Zhenglin Yang[g,1], Henry Ferreyra[c], Dirk-Uwe Bartsch[c], Igor Kozak[c], Liangfang Zhang[h], Feng Lin[e], Hui Sun[i], Hong Feng[j,1], and Kang Zhang[a,b,c,1]

[a]Molecular Medicine Research Center and Department of Ophthalmology, State Key Laboratory of Biotherapy, West China Hospital, Sichuan University, Chengdu, Sichuan 610064, China; [b]Institute for Genomic Medicine, and [c]Shiley Eye Center, University of California, La Jolla, CA 92093; [d]North Carolina Macular Consultants, Winston-Salem, NC 27103; [e]Department of Pathology, Case Western Reserve University, Cleveland, OH 44106; [f]ShengJing Affiliated Hospital of China Medical University, Shengyang, Liaoning 110004, China; [g]Institute of Laboratory Medicine, Sichuan Academy of Medical Sciences and Sichuan Provincial People's Hospital, Chengdu, Sichuan 610072, China; [h]Department of Nanoengineering, University of California at San Diego, La Jolla, CA 92093; [i]Department of Physiology, University of California, Los Angeles, CA 90095; and [j]Fengtian Hospital, Shengyang Medical College, Shengyang, Liaoning 110024, China

Edited* by Jonathan G. Seidman, Harvard Medical School, Boston, MA, and approved June 8, 2012 (received for review January 20, 2012)

The *rs1061170T/C* variant encoding the Y402H change in complement factor H (CFH) has been identified by genome-wide association studies as being significantly associated with age-related macular degeneration (AMD). However, the precise mechanism by which this CFH variant impacts the risk of AMD remains largely unknown. Oxidative stress plays an important role in many aging diseases, including cardiovascular disease and AMD. A large amount of oxidized phospholipids (oxPLs) are generated in the eye because of sunlight exposure and high oxygen content. OxPLs bind to the retinal pigment epithelium and macrophages and strongly activate downstream inflammatory cascades. We hypothesize that CFH may impact the risk of AMD by modulating oxidative stress. Here we demonstrate that CFH binds to oxPLs. The CFH 402Y variant of the protective *rs1061170* genotype binds oxPLs with a higher affinity and exhibits a stronger inhibitory effect on the binding of oxPLs to retinal pigment epithelium and macrophages. In addition, plasma from non-AMD subjects with the protective genotype has a lower level of systemic oxidative stress measured by oxPLs per apolipoprotein B (oxPLs/apoB). We also show that oxPL stimulation increases expression of genes involved in macrophage infiltration, inflammation, and neovascularization in the eye. OxPLs colocalize with CFH in drusen in the human AMD eye. Subretinal injection of oxPLs induces choroidal neovascularization in mice. In addition, we show that the CFH risk allele confers higher complement activation and cell lysis activity. Together, these findings suggest that CFH influences AMD risk by modulating oxidative stress, inflammation, and abnormal angiogenesis.

Genome-wide association studies have catalyzed significant progress in elucidating the molecular basis of complex trait diseases (1). However, a substantial gap remains in our understanding of how genetic variants contribute to disease. The complement factor H (CFH) locus for age-related macular degeneration (AMD) illustrates this challenge. AMD affects tens of millions of people worldwide and is the leading cause of irreversible blindness among the elderly on three continents. Most severe vision loss in AMD patients is caused by bleeding and exudation caused by choroidal neovascularization (CNV, also known as "wet AMD"). One of the best-replicated genetic associations is between CFH and AMD. The SNP variant *rs1061170*, which causes a tyrosine to histidine amino acid residue change (Y402H) in CFH, confers a significant risk for AMD and was present in more than 50% of AMD patients (2–6).

Oxidative stress has been associated with many aging disorders, including Alzheimer's disease, atherosclerosis, and AMD (7–11). It has been demonstrated that oxidative stress and oxidation products can result in inflammation and contribute significantly to the development of atherosclerotic lesions and macrophage activation (10, 12). For this reason the oxidized phospholipid (oxPL) level has been recognized as a reliable biomarker for evaluation of oxidative stress (13, 14). In the eye, a large amount of oxPLs are generated as the result of sunlight exposure and high oxygen content, and they initiate inflammation by binding to retinal pigment epithelium (RPE) and macrophages and activating downstream inflammatory cascades (15). In addition, oxidation-modified proteins and lipids have been detected in drusen and Bruch's membrane using Western blot analysis and immunohistochemistry (16).

The retinal photoreceptors are highly enriched with polyunsaturated fatty acid phospholipids such as phosphatidylcholine (PtC). These phospholipids are highly susceptible to oxidative stress, which can modify phospholipids and generate a variety of breakdown products to form oxPLs (17). Under oxidative modification, the head group of PtC, phosphocholine (PC), undergoes a conformational change exemplified by the oxidation of 1-palmitoyl-2-arachidonoyl-*sn*-glycero-3-phosphocholine (PAPC), one of the most common phospholipids in membrane structures, into 1-palmitoyl-2-(5′-oxo-valeroyl)-*sn*-glycero-3-phosphocholine (POVPC) (Fig. S1). This oxidation epitope can be recognized by a natural antibody to PC, TEPC-15 (also known as "T15") (Fig. S2). As a part of the innate defense system, T15 recognizes and interacts with PC on the cell wall of certain bacteria, such as *Streptococcus pneumococci*, to protect the host from lethal infection (17). However, T15 does not bind to PC on normal cell membranes or lipoproteins unless they have been oxidatively modified, such as oxPLs on low-density lipoprotein (oxLDL) or in the cell membrane of apoptotic cells. These properties of T15 make it a useful tool for studying oxPLs in diseases such as atherosclerotic lesion development, a condition that shares similarities with drusen development in AMD (15, 18). Recent

Author contributions: P.X.S. and K.Z. designed research; P.X.S., Li Zhang, M.Z., H.D., L. Zhao, C.L., S.G., S.L.L., G.H., J. Lee, M.B., M.H.N., F. Lu, M.K., J. Luo, H.O., Z.T., Z.S., J.Z., X.W., Z.F., Y.D., Z.Y., H. Ferreyra, D.-U.B., I.K., Liangfang Zhang, F. Lin, and H. Feng performed research; P.X.S., Li Zhang, H.S., and K.Z. analyzed data; and P.X.S. and K.Z. wrote the paper.

The authors declare no conflict of interest.

*This Direct Submission article had a prearranged editor.

[1]To whom correspondence may be addressed: kang.zhang@gmail.com, zliny@yahoo.com, or fenghongcn@hotmail.com.

This article contains supporting information online at www.pnas.org/lookup/suppl/doi:10.1073/pnas.1121309109/-/DCSupplemental.

studies revealed that natural antibodies also bind to modified cellular and molecular structures caused by endogenous oxidative damage. These interactions can mask offensive macromolecules such as apoptotic cells and oxLDL and facilitate the turnover of unhealthy cells to maintain homeostasis (13, 17).

CFH is also a component of the innate immune system and is a major regulator of the complement system. CFH binds to bacteria through certain bacterial polysaccharides, lipids, or proteins via recognition of pathogen-associated molecular patterns (PAMPs) (19). We have reported previously that CFH binds to M6 protein of *Streptococcus pyogenes* (20). In addition to recognizing PAMPs on bacteria, we speculated that CFH also could interact with the damage-associated molecular patterns (DAMPs) generated by endogenous oxidative stress to shield the unnecessary cytolytic events.

Given the functional similarities between CFH and natural antibodies—both are elements of the innate defense system modulating a variety of exogenous insults and endogenous structural modification—and a strong genetic association between CFH and AMD, we hypothesized that a function of CFH is to modulate inflammation through binding oxidation-specific epitopes (e.g., oxPLs). In this report, we investigated the differential binding of CFH402Y/H variants to oxidation epitopes derived from phospholipid oxidation and its consequent impact on inflammation and complement activation. Our results suggest that CFH influences AMD risk by binding to oxPLs and modulating oxidative stress, inflammation, and abnormal angiogenesis.

Results

We first observed that, regardless of genotypes, CFH exhibited significantly higher binding toward oxLDL than toward native LDL (nat-LDL) (Fig. 1*A*), indicating that CFH binds to oxPLs rather than unmodified phospholipids on LDL. The average relative binding as expressed in relative light units (RLU) was 132,060 ± 5,175 for oxLDL and only 25,424 ± 889 for nat-LDL ($P = 5.59 \times 10^{-67}$). We then compared binding of the risk (*C*) and protective (*T*) alleles of *rs1061170* in plasma CFH. When assayed under the same conditions, plasma CFH from *rs1061170* homozygous *CC* (402H, risk genotype) subjects displayed lower binding to oxLDL than plasma CFH from heterozygous *CT* or homozygous *TT* (402Y, protective genotypes) subjects (Fig. 1*B*). The differential binding of CFH402Y and CFH402H to the oxidation epitopes was confirmed further by ELISA using recombinant CFH402Y and CFH402H proteins. Specifically, we showed that CFH402Y bound to both POVPC-BSA and oxLDL almost twice as strongly as CFH402H (Fig. 1*C*).

We next tested whether plasma level of oxPLs per apolipoprotein B (oxPLs/apoB), a reliable biomarker for systemic oxidative stress (14, 21), is correlated with CFH genotypes. We measured plasma oxPLs/apoB levels from non-AMD subjects with different *rs1061170* genotypes. Plasma with a *CC* risk genotype had a higher level of oxPLs/apoB than plasma with protective genotypes (Fig. 1*D*), suggesting that the binding affinity of CHF for oxPLs correlates inversely with plasma levels of oxPLs. Because CFH is a major negative regulator of complement activation, we tested whether there was a difference in complement-mediated cell lysis modulated by CFH proteins encoded by the *rs1061170* risk genotype (*CC*, $n = 34$) and the protective genotype (*TT*, $n = 40$). There was a 25% increase in final complement-mediated cell lysis associated with the *CC* genotype compared with that associated with the *TT* genotype (Fig. 1*E*).

RPE and macrophages share many similar biological features such as binding and phagocytosis of oxLDL via cell-surface receptors, including CD36 (22, 23). These processes can lead to intracellular accumulation of debris and lipofuscin and induction of cytokines critical for activation of proinflammatory cascades and consequent abnormal angiogenesis. We therefore surveyed gene-expression profiles in cultured RPE and macrophage cell lines upon exposure to oxLDL. We found up-regulation of CCR2, CD36, IL-8, TNF, and VEGF in RPE upon incubation with

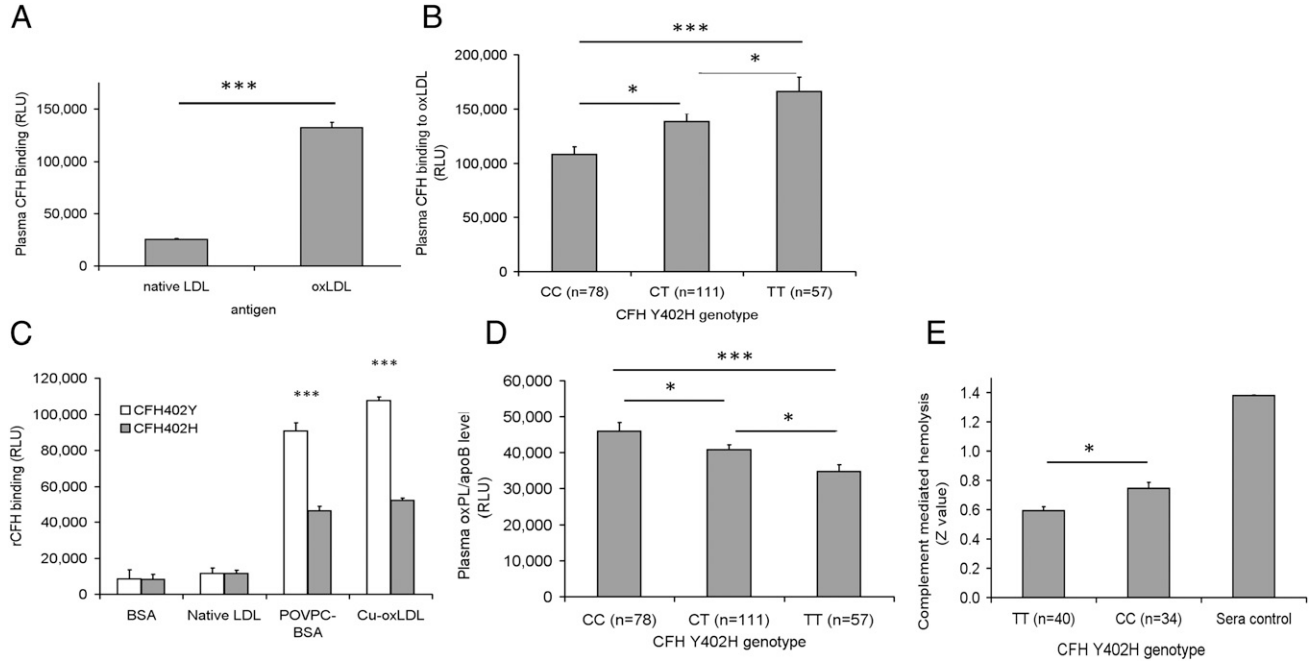

Fig. 1. (*A*) Plasma CFH binds preferentially to oxLDL rather than to native LDL. (*B*) Plasma CFH binding to oxLDL stratified by Y402H genotypes. (*C*) Differential binding of recombinant CFH402Y and CFH402H to oxidative epitopes of POVPC and oxLDL with BSA and native LDL as controls. Data are expressed in RLU and as mean ± SEM. ***$P < 0.001$. (*D*) Plasma oxPLs/apoB level detected by anti-PC antibody T15 stratified by CFHY492H genotypes. (*E*) Complement-mediated hemolysis stratified by CFH Y402H genotypes. Heat-inactivated normal human sera that contained inactive CFH were used as a negative control for complement activation inhibition. Data are shown as *Z* values and as mean ± SEM.

oxLDL (Fig. 2*A*). CCR2 is a receptor for monocyte chemoattractant protein 1 (MCP-1). MCP-1 is an important factor in recruiting circulating monocytes to the subretinal space and promoting the monocytes to differentiate into resident macrophages. IL-8 is an inflammatory cytokine that has been shown to be specifically associated with oxidative stress (24). We also found up-regulation of CD36, IL-6, and VEGF by oxLDL in macrophages (Fig. 2*B*). Because binding of oxLDL to RPE and macrophages led to increased expression of proinflammatory and proangiogenic genes, CFH binding to oxLDL may protect against CNV development. We next tested whether CFH can inhibit binding of oxLDL to RPE and macrophages. Cultured RPE cells and macrophages were exposed to oxLDL in the presence of CFH proteins encoded by either the *rs1061170* risk (*C*) or protective (*T*) allele. We found that CFH encoded by the protective (*T*) allele (402Y) exhibited a stronger inhibitory effect on binding of oxLDL to RPE (Fig. 2*C*) and macrophages (Fig. 2*D*) than seen with CFH encoded by the risk (*C*) allele (402H). Our result suggests that CFH protein encoded by the protective allele has a stronger inhibitory effect on oxLDL binding to RPE and macrophages, indicating a role of CFH in reducing oxidative stress.

To test whether oxLDL is sufficient to cause AMD-like features in vivo, we injected oxLDL into the subretinal space in 2-mo-old normal C57BL/6 mice. We found exudation and leakage characteristic of CNV on fundus fluorescein angiography and indocyanine green (ICG) angiography (Fig. S3). Histological analysis showed marked CNV in injection sites (Fig. 3*A*). Consistent with the gene-expression profile in cell-culture experiments (Fig. 2 *A* and *B*), we found macrophage infiltration (Fig. 3*B*), VEGF expression (Fig. 3 *E* and *I*), and abnormal angiogenesis in the CNV lesions (Fig. 3 *D*–*J*). Drusen are a hallmark of AMD and have been shown to accumulate CFH. Consistent with a role of oxidative stress in human AMD pathogenesis, we found immunolabeling of oxPL epitopes colocalized with CFH staining in drusen and Bruch's membrane in a human AMD eye (Fig. 4).

Discussion

Extensive genetic association studies suggest that the disease-associated genotype of CFH *rs1061170* confers a major risk for developing AMD (2–5). At the same time, the mechanism by which these CFH genotypes contribute to the risk of AMD is largely unknown. In this study, we showed that CFH reduces oxidative stress by binding to oxPLs, thus preventing oxPLs from activating inflammatory cascades in RPE and macrophages and from subsequently reducing abnormal angiogenesis.

It has been postulated for some time that oxidative stress plays a critical role in AMD pathogenesis (9, 10). The outer segments of retinal photoreceptors possess the highest content of polyunsaturated fatty acids (PUFAs) in the body, and these PUFAs undergo rapid turnover once every 2 wk (25, 26), releasing a large amount of PUFA-containing membrane fragments. These PUFAs are subject to strong oxidative stress because of exposure to high oxygen content in the outer retina and to sunlight, often exacerbated by smoking. It is possible that a significant amount of oxidation products such as oxPL-containing lipids or protein adducts are taken up by the RPE, presumably through receptors such as CD36. These products are strong inflammatory stimulants and monocyte chemoattractants (Fig. 2*A*), and they attract and recruit circulating monocytes and promote resident macrophage differentiation. These oxidation products also can stimulate macrophages to express CD36, leading to phagocytosis of oxidized lipids and proteins. The oxidized lipid and protein-filled macrophages may further exacerbate inflammation, similar to the action of those described in our in vitro experiments (Fig.

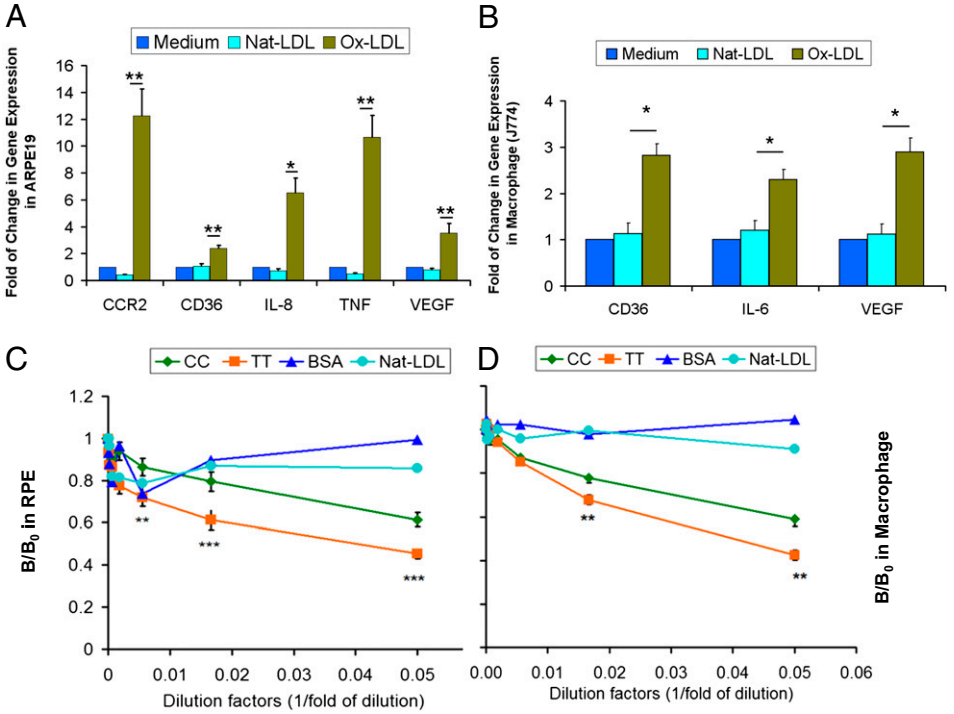

Fig. 2. (*A* and *B*) Gene expression as assayed by quantitative PCR on RNA from ARPE19 (*A*) or J774 (*B*) macrophages treated with 50 μg/mL of oxLDL for 6 h. Relative mRNA levels were calculated by normalizing results with *GAPDH* and are expressed relative to untreated samples. $n = 4$. (*C* and *D*) Inhibition of binding of oxLDL to RPE (*C*) and J774 (*D*) macrophages by CFH *rs1061170* (Y402H) alleles. Cultured RPE or mouse J774 macrophages were incubated with biotin-oxLDL premixed with serial dilutions of plasma of the CFH *CC* (risk) allele (402H, $n = 7$) or the *TT* (protective) allele (402Y, $n = 7$) genotypes. The biotin-oxLDL bond was detected with NeutrAvidin-AP. The data are expressed as the ratio of B/B_0, where B is binding with CFH and B_0 is binding without CFH as a competitor. Nat-LDL was used as a negative control. Data are shown as mean ± SEM. $^*P < 0.05$; $^{**}P < 0.01$; $^{***}P < 0.001$.

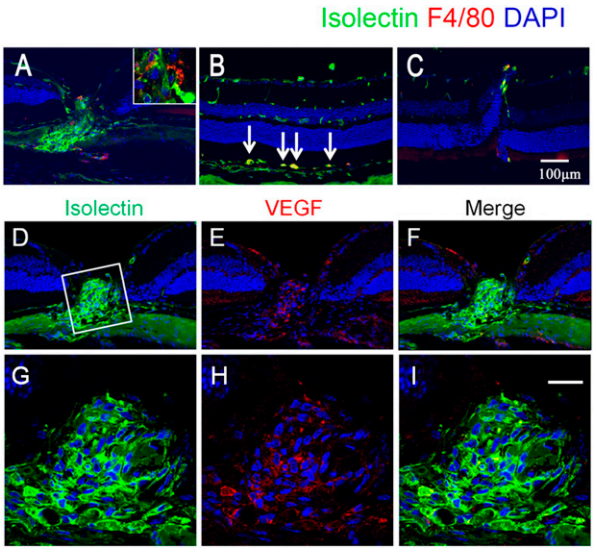

Fig. 3. (*A–C*) Induction of CNV by subretinal injection of oxLDL. (*A*) Following subretinal injection of oxLDL, marked neovascularization was found in an injection site. (*B*) Subretinal injection of oxLDL also induced increased vascular activity in the subretinal space, which was closely associated with F4/80-positive macrophages (arrows). Vascularity activity was visualized with isolectin staining (green), and macrophages were visualized with F4/80 staining (red). Cell nuclei were counterstained with DAPI (blue). (*C*) As a negative control, nat-LDL injection did not promote CNV or macrophage activation. (*D–I*) Localization of VEGF in CNV. Double labeling of neovascularization by isolectin (green, *D* and *G*), and VEGF (red, *E* and *H*) demonstrates that VEGF was localized within a neovascular complex. *G*, *H*, and *I* show magnified images of the boxed area in *D*. (Scale bars: 100 μm.)

2*B*) and of foam cells in atherosclerotic lesions (15, 22, 27, 28). Inflammation can lead to the production of VEGF and angiogenesis. Our results suggest a mechanism by which oxidative stress on photoreceptor cells generates oxidation-specific epitopes that promote and amplify the inflammation and angiogenic response in RPE and macrophages.

Recently, Weismann and coworkers (29) reported a link between CFH and oxidative stress in AMD. They described

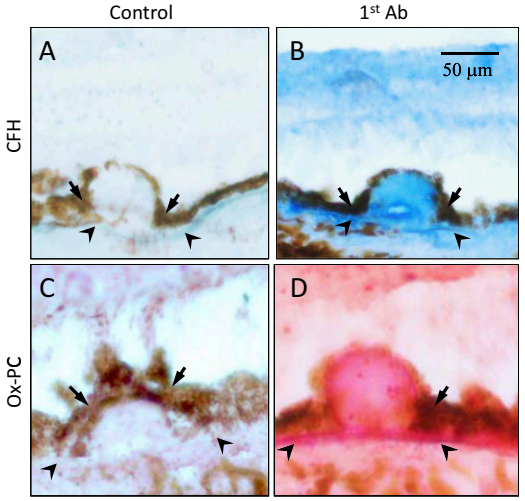

Fig. 4. Colocalization of oxPC with CFH in human AMD lesions. Immunohistochemistry of serial sections of an AMD eye stained with antibodies to CFH (*B*, blue color) or oxPC (*D*, pink color). Omission of the first antibody served as a negative control (*A* and *C*). (Scale bar: 50 μm.)

a differential binding of CFH *rs1061170* variants to LDL conjugated with malondialdehyde (MDA, CHO-CH_2-CHO) or malondialdehyde-acetaldehyde (MAA), providing another line of evidence for the involvement of CFH in protection against oxidative stress. In their study, copper oxLDL (cu-oxLDL) was not able to compete effectively with the binding of MDA- or MAA-conjugated LDL to CFH. It is possible that there is a stronger interaction between CFH and MDA/MAA-LDL than between CFH and cu-oxLDL. However, the amount of oxLDL in human plasma is more relevant to an in vivo oxidative stress level, as demonstrated by its extensive use in cardiovascular research (14), where the development of atherosclerotic lesions in arterial wall has strong similarity to the development of drusen in AMD eyes (15, 18, 28). The oxPLs on cu-oxLDL defined by the T15 antibody have been shown to be a major stimulant to inflammation (27, 30). We believe that the cu-oxLDL described in our current study appropriately represents in vivo oxPLs in the context of chronic diseases such as AMD.

Our results showed that CFH binding to oxPLs prevents the binding of oxPLs to RPE and macrophages, thereby inhibiting inflammation and abnormal angiogenesis. Because CFH is one of the most abundant plasma proteins, it may play a major role in controlling systemic oxidative burden, which in turn influences the risk of AMD in concert with the local oxidative stress in the eye.

As an important regulator of the complement pathway, CFH has been shown to be associated with various diseases (31). Multiple variants of CFH have been identified as contributing to the pathogenesis of diseases such as hemolytic uremic syndrome, thrombotic thrombocytopenic purpura (32), glomerulonephritis (33), intracerebral hemorrhage (34), lung cancer (35), and sudden sensorineural hearing loss (36). Thus, far, variants of CFH that have been associated directly with AMD risk include Y402H, I62V (37–39), and R1210C (40). In this study, we attempted to elucidate the functional consequences of the CFH 402 Y to H change. We showed that the change affects the binding properties of CFH to oxPLs and compromises its ability to shield these DAMPs. Studies indicate that even mild forms of oxidized lipoproteins (e.g., minimally modified LDL) can cause changes in gene expression (e.g., activating NFκB-like factors) in vascular cells that subsequently lead to the initiation and maintenance of an inflammatory response (41). Our study also demonstrated that plasma from a protective CFH homozygous *rs1061170* genotype has stronger protection against complement-mediated hemolysis.

It is clear that we have just begun to understand the complicated interplay between genetic predisposition and environmental risk factors, such as oxidative stress, and the impact of this interplay on AMD pathogenesis. Further investigation of downstream events, such as the clearance of CFH-bound oxPLs as well as other possible outcomes and pathways involved, would provide a more thorough understanding of the etiology of AMD. In summary, our study suggests the involvement of oxPLs in AMD and a role for CFH in modulating such an interaction. Determination of predisposed genetic risk in combination with oxPL biomarkers may allow early intervention and preventive treatment of AMD.

Materials and Methods

Study Subjects. This study was approved by the Institutional Review Boards of the West China Hospital of Sichuan University and the University of California at San Diego. Subjects gave informed consent before participation. All participants underwent a standard examination, including visual acuity measurements, dilated slit-lamp biomicroscopy, and color fundus photography and fluorescein angiography. Diagnosis of wet AMD was based on the presence of CNV with the classification established by the Age-Related Eye Disease Study (AREDS (equivalent to AREDS category 4) (42). Blood samples were taken by venipuncture without fasting. Genomic DNA was extracted from peripheral blood mononuclear cells, and plasma was stored at −20 °C until use. For the biomarker ELISA study, we used plasma from non-AMD

subjects to avoid a bias in a systemic oxidative stress level caused by oral intake of "eye vitamins" widely prescribed to AMD patients.

Genotyping. CFH SNP *rs1061170* (Y402H) was genotyped by SNaPshot according to published methods (43), using an ABI 3130XL analyzer (ABI) according to the manufacturer's instructions. All SNPs had a genotyping success rate >99.9% and accuracy >99% as judged by random resequencing of 20% of samples.

Preparation of Native and Oxidized Phospholipids. POVPC was purchased from Avanti Polar Lipids and was covalently conjugated to BSA as previously described (44). Because phospholipids have low aqueous solubility, in plasma they typically coexist with proteins in the form of lipoproteins, such as ApoB in LDL. We thus chose LDL as a carrier for native phospholipids and oxPL in this study. We first isolated LDL from plasma of normolipidemic donors by sequential ultracentrifugation (45). OxLDL was generated by incubating LDL (1 mg/mL) with an oxidation agent (10 μM CuSO4) for 18 h at 37 °C; native phospholipids on the surface of LDL were oxidized into oxPL (46). Native (unoxidized) phospholipids on nat-LDL were used as a control. After preparation, both nat-LDL and oxLDL were dialyzed with PBS containing 0.27 mM EDTA to prevent further oxidation.

Production of Recombinant CFH402Y and CFH402H. cDNA encoding human CFH402Y and CFH402H was subcloned into a mammalian expression vector pRK5. The constructs then were transfected into HEK293 cells using Fugene 6 kit following the manufacturer's instruction (Roche). The medium containing CFH402Y or CFH402H protein was harvested and concentrated using Amicon Ultra (Millipore).

ELISA. Monoclonal antibodies to oxidized PC (oxPC), TEPC-15 (T15), and rabbit anti-CFH IgG were purchased from Sigma. For an ELISA, 2 μg/mL of antigens (in PBS) were coated on microtiter plates at 4 °C overnight. A 1:100 dilution of plasma was added to the plate, followed by biotinylated anti-CFH antibody. The antigen concentration and plasma dilution factors were determined by a preliminary experiment (Fig. S4). The amount of bound CFH was detected with neutral avidin-alkaline phosphatase (AP) followed by light emission substrate Lumiphos 530. The chemiluminescence was measured by GloMax Luminetor (Promega) and expressed as RLU. OxPLs/apoB was measured as previously described (14). Laboratory staff who evaluated the results were masked to the type of plasma and other relevant variables to avoid bias.

Binding Assay of oxLDL to RPE and Macrophages. Human RPE cell lines (ARPE19) or mouse macrophage cell lines (J774) were grown on microtiter plates and applied with biotin-oxLDL premixed with serial dilutions of plasma of different CFH genotypes. After unbound biotin-oxLDL was washed away, the remaining biotin-oxLDL was detected with NeutrAvidin-AP (Thermo Scientific, Rockford, IL). The data were expressed as B/B_0, where B is binding with CFH and B_0 is binding without CFH as a competitor. Nat-LDL and BSA were used as negative controls.

Complement Activation Assay. CFH inhibitory activity in plasma stratified by CFHY402H genotype was assessed by a modified sheep erythrocytes-based hemolytic assay as described previously (47). Briefly, 4×10^6 sheep erythrocytes were mixed with 30% (vol/vol) factor H-depleted serum in EGTA/Mg^{2+} buffer in a 100-μL volume with 1:50 diluted heat-inactivated plasma of different genotypes and then were incubated for 30 min at 37 °C. Complement-mediated hemolysis was quantitated by measuring OD_{405} after centrifugation, and the average number of lytic sites per blood cell (Z value) of sample x was calculated using equation: $z = -\ln\{1 - [(OD_{405}(x) - OD_{405}(0\%)]/[OD_{405}(100\%) - OD_{405}(0\%)]\}$, in which OD_{405} (0%) represents incubation of sheep erythrocytes with 1 mM EDTA, and OD_{405} (100%) represents incubation of sheep erythrocytes with H_2O (48).

Mouse Subretinal Injection of oxLDL and Immunohistochemistry. Two-month-old C57BL/6 mice were given 2 μL of oxLDL at 50 μg/mL in one eye via subretinal injection. At the same time point the fellow eye was given a subretinal injection of 2 μL nat-LDL at 50 μg/mL or PBS as negative control. A successful injection was ascertained by the creation of a small subretinal bleb. All mice underwent fluorescein angiography and were then killed 6 wk after injection. Eyes were enucleated immediately and fixed for 30 min in 4% (vol/vol) paraformaldehyde. Twelve-micrometer cryostat sections were incubated in primary antibodies F4/80 (Invitrogen) or anti-mouse Vegf antibody (Sigma) and were detected with a Texas Red-conjugated secondary antibody (Invitrogen,). The same section also was incubated with FITC-conjugated isolectin to stain for blood vessels (Sigma). Images were captured on a Zeiss 510 confocal microscope.

Fluorescein Angiography and Indocyanine Green Angiography. Six weeks after subretinal injection, mice were anesthetized by s.c. injection of ketamine (60 mg/kg) and xylazine (10 mg/kg), and their pupils were dilated. Infrared images of the retinal fundus were taken before dye injection. All mice had fluorescein and ICG angiography examinations using a confocal scanning laser ophthalmoscope (Heidelberg Engineering). Injections of 25 mg/kg of ICG and 1 mL/kg of 10% (vol/vol) fluorescein solution were given i.v. via a sublingual vein. Filling phases were captured and stored for review.

Immunohistochemistry of Human Drusen. An eye from an 85-y-old male AMD donor was used in the study of the immunohistochemistry of human drusen. The AMD eye was fixed in 4% (vol/vol) paraformaldehyde and then was cryopreserved in OCT medium. The fixed eye was sectioned to a thickness of 6 μM. Immunohistochemistry was performed using 5 μg/mL rabbit anti-human CFH IgG antibody (Sigma) or 5 μg/mL monoclonal anti-oxPC mouse IgA antibody T15 (Sigma). Anti-rabbit IgG (whole molecule) AP conjugate (Sigma) or anti-mouse IgA peroxidase conjugate (Vector Labs) was used as the secondary antibody. The VectorStain Elite ABC kit and the alkaline phosphatase substrate kit (Vector Labs) were used for CFH detection, and the VectorStain Quick kit and the VIP peroxidase substrate kit (Vector Labs) were used for oxPC detection. Immunolabeling was captured using Zeiss Observer A1 microscopy.

Real-Time Quantitative PCR. Total RNA was extracted from cell cultures using the RNeasy Mini Kit from QIAGEN and was converted to cDNA using the SuperScript III First Strand Synthesis System (Invitrogen). All quantitative RT-PCR experiments were performed with Power SYBR Green qPCR Master Mix from Applied Biosystems and MyiQ Single Color Real-Time PCR Detection System from Bio-Rad Laboratories. Primer sets used are listed in Table S1. Relative mRNA levels were calculated by normalizing results with GAPDH and are expressed relative to untreated samples.

Data Analysis. The Student's t test was performed to evaluate the difference in binding of *CFH* alleles to oxLDL or nat-LDL. $P < 0.05$ was considered significant (*). $P < 0.01$ (**) or $P < 0.001$ (***) was considered very significant.

ACKNOWLEDGMENTS. We thank members of the K.Z. laboratory for assistance and helpful discussions. This work is supported by grants from the Natural Science Foundation of China (Grant 81130017 to K.Z. and Grant 81025006 to Z.Y.), the National Basic Research Program of China (973 Program, 2011CB510200 to K.Z.). K.Z. is also supported by the National Eye Institute/National Institutes of Health, the King Abdulaziz City for Science and Technology through the UC San Diego Center of Excellence in Nanomedicine center grant, a Veterans Affairs Merit Award, Research to Prevent Blindness, and a Burroughs Wellcome Fund Clinical Scientist Award in Translational Research.

1. Manolio TA, Brooks LD, Collins FS (2008) A HapMap harvest of insights into the genetics of common disease. *J Clin Invest* 118:1590–1605.
2. Klein RJ, et al. (2005) Complement factor H polymorphism in age-related macular degeneration. *Science* 308:385–389.
3. Haines JL, et al. (2005) Complement factor H variant increases the risk of age-related macular degeneration. *Science* 308:419–421.
4. Hageman GS, et al. (2005) A common haplotype in the complement regulatory gene factor H (HF1/CFH) predisposes individuals to age-related macular degeneration. *Proc Natl Acad Sci USA* 102:7227–7232.
5. Edwards AO, et al. (2005) Complement factor H polymorphism and age-related macular degeneration. *Science* 308:421–424.
6. Magnusson KP, et al. (2006) CFH Y402H confers similar risk of soft drusen and both forms of advanced AMD. *PLoS Med* 3:e5.
7. Binder CJ, et al. (2002) Innate and acquired immunity in atherogenesis. *Nat Med* 8:1218–1226.
8. Brewer GJ (2007) Iron and copper toxicity in diseases of aging, particularly atherosclerosis and Alzheimer's disease. *Exp Biol Med (Maywood)* 232:323–335.
9. Beatty S, Koh H, Phil M, Henson D, Boulton M (2000) The role of oxidative stress in the pathogenesis of age-related macular degeneration. *Surv Ophthalmol* 45:115–134.
10. Hollyfield JG, et al. (2008) Oxidative damage-induced inflammation initiates age-related macular degeneration. *Nat Med* 14:194–198.
11. Seddon JM, George S, Rosner B (2006) Cigarette smoking, fish consumption, omega-3 fatty acid intake, and associations with age-related macular degeneration: The US Twin Study of Age-Related Macular Degeneration. *Arch Ophthalmol* 124:995–1001.
12. Chou MY, et al. (2009) Oxidation-specific epitopes are dominant targets of innate natural antibodies in mice and humans. *J Clin Invest* 119:1335–1349.

13. Chou MY, et al. (2008) Oxidation-specific epitopes are important targets of innate immunity. *J Intern Med* 263:479–488.
14. Tsimikas S, et al. (2005) Oxidized phospholipids, Lp(a) lipoprotein, and coronary artery disease. *N Engl J Med* 353:46–57.
15. Curcio CA, Johnson M, Huang JD, Rudolf M (2010) Apolipoprotein B-containing lipoproteins in retinal aging and age-related macular degeneration. *J Lipid Res* 51: 451–467.
16. Crabb JW, et al. (2002) Drusen proteome analysis: An approach to the etiology of age-related macular degeneration. *Proc Natl Acad Sci USA* 99:14682–14687.
17. Shaw PX, et al. (2000) Natural antibodies with the T15 idiotype may act in atherosclerosis, apoptotic clearance, and protective immunity. *J Clin Invest* 105:1731–1740.
18. Mullins RF, Russell SR, Anderson DH, Hageman GS (2000) Drusen associated with aging and age-related macular degeneration contain proteins common to extracellular deposits associated with atherosclerosis, elastosis, amyloidosis, and dense deposit disease. *FASEB J* 14:835–846.
19. Hazen SL (2008) Oxidized phospholipids as endogenous pattern recognition ligands in innate immunity. *J Biol Chem* 283:15527–15531.
20. Yu J, et al. (2007) Biochemical analysis of a common human polymorphism associated with age-related macular degeneration. *Biochemistry* 46:8451–8461.
21. Ahmadi N, et al. (2010) Relation of oxidative biomarkers, vascular dysfunction, and progression of coronary artery calcium. *Am J Cardiol* 105:459–466.
22. Sun M, et al. (2006) Light-induced oxidation of photoreceptor outer segment phospholipids generates ligands for CD36-mediated phagocytosis by retinal pigment epithelium: A potential mechanism for modulating outer segment phagocytosis under oxidant stress conditions. *J Biol Chem* 281:4222–4230.
23. Boullier A, et al. (2001) Scavenger receptors, oxidized LDL, and atherosclerosis. *Ann N Y Acad Sci* 947(1):214–222; discussion 222–213.
24. Vlahopoulos S, Boldogh I, Casola A, Brasier AR (1999) Nuclear factor-kappaB-dependent induction of interleukin-8 gene expression by tumor necrosis factor alpha: Evidence for an antioxidant sensitive activating pathway distinct from nuclear translocation. *Blood* 94:1878–1889.
25. Young RW (1967) The renewal of photoreceptor cell outer segments. *J Cell Biol* 33: 61–72.
26. Young RW (1971) The renewal of rod and cone outer segments in the rhesus monkey. *J Cell Biol* 49:303–318.
27. Miller YI, et al. (2011) Oxidation-specific epitopes are danger-associated molecular patterns recognized by pattern recognition receptors of innate immunity. *Circ Res* 108:235–248.
28. Seddon JM, George S, Rosner B, Rifai N (2005) Progression of age-related macular degeneration: Prospective assessment of C-reactive protein, interleukin 6, and other cardiovascular biomarkers. *Arch Ophthalmol* 123:774–782.
29. Weismann D, et al. (2011) Complement factor H binds malondialdehyde epitopes and protects from oxidative stress. *Nature* 478:76–81.
30. Miller YI, Chang MK, Binder CJ, Shaw PX, Witztum JL (2003) Oxidized low density lipoprotein and innate immune receptors. *Curr Opin Lipidol* 14:437–445.
31. Boon CJ, et al. (2009) The spectrum of phenotypes caused by variants in the CFH gene. *Mol Immunol* 46:1573–1594.
32. Kavanagh D, Goodship TH, Richards A (2006) Atypical haemolytic uraemic syndrome. *Br Med Bull* 77-78:5–22.
33. Schejbel L, et al. (2011) Complement factor H deficiency and endocapillary glomerulonephritis due to paternal isodisomy and a novel factor H mutation. *Genes Immun* 12:90–99.
34. Appelboom G, et al. (2011) Complement Factor H Y402H polymorphism is associated with an increased risk of mortality after intracerebral hemorrhage. *J Clin Neurosci* 18: 1439–1443.
35. Cui T, et al. (2011) Human complement factor H is a novel diagnostic marker for lung adenocarcinoma. *Int J Oncol* 39:161–168.
36. Nishio N, et al. (2012) Contribution of complement factor H Y402H polymorphism to sudden sensorineural hearing loss risk and possible interaction with diabetes. *Gene* 499:226–230.
37. Maller J, et al. (2006) Common variation in three genes, including a noncoding variant in CFH, strongly influences risk of age-related macular degeneration. *Nat Genet* 38: 1055–1059.
38. Kondo N, Honda S, Kuno S, Negi A (2009) Coding variant I62V in the complement factor H gene is strongly associated with polypoidal choroidal vasculopathy. *Ophthalmology* 116:304–310.
39. Xing C, et al. (2008) Complement factor H polymorphisms, renal phenotypes and age-related macular degeneration: The Blue Mountains Eye Study. *Genes Immun* 9: 231–239.
40. Raychaudhuri S, et al. (2011) A rare penetrant mutation in CFH confers high risk of age-related macular degeneration. *Nat Genet* 43:1232–1236.
41. Berliner JA, et al. (1995) Atherosclerosis: Basic mechanisms. Oxidation, inflammation, and genetics. *Circulation* 91:2488–2496.
42. Age-Related Eye Disease Study Research Group (1999) The Age-Related Eye Disease Study (AREDS): Design implications. AREDS report no. 1. *Control Clin Trials* 20: 573–600.
43. Yang Z, et al. (2008) Toll-like receptor 3 and geographic atrophy in age-related macular degeneration. *N Engl J Med* 359:1456–1463.
44. Pégorier S, Stengel D, Durand H, Croset M, Ninio E (2006) Oxidized phospholipid: POVPC binds to platelet-activating-factor receptor on human macrophages. Implications in atherosclerosis. *Atherosclerosis* 188:433–443.
45. Havel RJ, Eder HA, Bragdon JH (1955) The distribution and chemical composition of ultracentrifugally separated lipoproteins in human serum. *J Clin Invest* 34:1345–1353.
46. Palinski W, et al. (1990) Antisera and monoclonal antibodies specific for epitopes generated during oxidative modification of low density lipoprotein. *Arteriosclerosis* 10:325–335.
47. Zipfel PF, et al. (2007) Deletion of complement factor H-related genes CFHR1 and CFHR3 is associated with atypical hemolytic uremic syndrome. *PLoS Genet* 3:e41.
48. Fearon DT, Austen KF, Ruddy S (1973) Formation of a hemolytically active cellular intermediate by the interaction between properdin factors B and D and the activated third component of complement. *J Exp Med* 138:1305–1313.